

# Electromagnetics Finite Element Analysis for Designing High Frequency Inductive Position Sensors

Lidu Huang, Aziz Rahman, W. Donald Rolph and Chris Pare

Texas Instruments, Inc., Materials & Controls Group

34 Forest Street, Attleboro, MA 02703, USA

*Abstract-- In this paper, we use a transient electromagnetic finite element analysis tool to design a non- contact inductive position sensor. The sensor's primary and secondary coils are laid on a printed circuit board. The primary coil is excited by a ramp current source, and the secondary output is measured for sensing purpose. A copper target is employed to detect the position of its movement. Electromagnetic finite element analysis results are applied in the designs, and are further verified by the measured results from prototyping. The numerical analysis results help us to understand the sensor's behavior, and to optimize its design.*

*Index Terms-- Eddy current, inductive sensor, position/ displacement sensor, transient electromagnetic finite element analysis*

## I. INTRODUCTION

Traditional electric contact position sensors and switches do not meet the demanding longer-life requirement due to the excessive mechanical contact wear. Non-contact position sensors using Hall effect, inductive and other techniques will become increasingly attractive. In this paper, we present an application of electromagnetic finite element method in designing a linear position sensor using high frequency inductive technique.

EMAS [1], an electromagnetic finite element analysis system, is one of the tools that we have utilized to reduce our development cycle and to improve product quality [2,3]. Electromagnetic finite element analysis makes it possible to visualize distributions of eddy current density and electro-magnetic fields, to extract RCL equivalent circuit parameters, and to obtain transient electromagnetic responses, such as induced current and potentials. As operating frequencies for sensors push higher and higher, crosstalk and ground bounce become greater concerns for sensor designers. High frequency electromagnetics finite element analysis has become an essential tool in new product development, allowing designs to be optimized prior to be prototyped.

The high frequency inductive position sensor in design uses several turns of primary and secondary coils on a printed circuit board. The primary coil is periodically excited by a ramp current source, which generates a rapid change of magnetic field and induces electric potential in the secondary coil. A schematic design diagram for an analog sensor is shown in figure 1, where primary and secondary coils are shown along with a shielding ground plane in the back and a moving target in the front. A manually actuated copper target is positioned in the proximity to the coil structure; the sensor output is proportional to the relative position of this target.

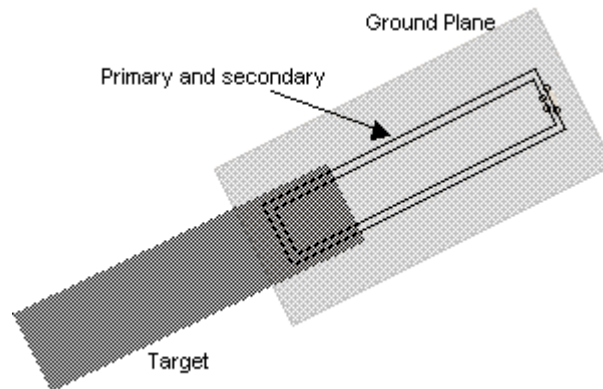


**Fig. 1 A schematic diagram for a linear inductive position sensor**

Since the copper target has a very small resistance, it is more efficient than the secondary coil in generating an induced magnetic field which opposes the induction field generated by the primary coil. With the target present, the secondary output is reduced, and within a certain operating range, the output is linearly proportional to the target coverage area.

## II. 3D TRANSIENT ELECTROMAGNETICS FEA

The objective of the 3D transient electromagnetic finite element analysis is to optimize the sensor design via a nonlinear design of experiments (DOE). For example, in order to maximize the output signal, the best combination for the numbers of turns of primary and secondary coils can be found numerically. Or, to minimize the output variation caused by the specified but unavoidable manufacturing tolerance, a safer separation distance between primary and secondary can be determined as well.

### A. Model

The transient electromagnetic finite element model consists of following:

- **Geometry:** the physical location and dimension of primary, secondary, ground plane, and target inside the model volume and air between and surrounding these electromagnetic components. A solid model in CAD might be a good starting point for setting up a useful 3D model. However, superfluous mechanical structures should be removed, and any part of the solid model that is made of non-electromagnetic materials can be treated as air to simplify the solid model. This would significantly simplify the solid model. Since air between and around the sensor elements also conducts electromagnetic field, it must be included in the model as well. In many cases, it's better to create geometry from scratch for electromagnetic analysis. This also has the advantage of allowing the analyst to create the geometric model parametrically. A parametric model is especially important for new product design, as the design evolves rapidly at its early development stage. Converting an updated CAD model to a useful geometry for finite element meshing demands almost the same amount of manual changes each time.
- **Material properties:** the behavior of materials when subjected to electromagnetic fields. Air, copper, and other associated electromagnetic materials are used in the finite element model. The material properties required for transient electromagnetic analysis are conductivity, permittivity, and permeability.
- **Finite element mesh:** composed of 3D elements and 1D wire elements within the model volume. The 1D line elements, which represents the primary and secondary coils, are constructed manually. A typical finite element model for this type of analysis consists of about 34,000 hexahedral elements with nearly 37,000 grid points. The problem has about 148,000 degrees of freedom.
- **Boundary condition:** the behavior outside the model volume. In this analysis, the magnetic field is required to be tangent to all outer boundaries. For the electric boundary condition, one end of the primary coil is grounded, while the other end is excited by a point current source.
- **Excitations:** the input energy to the sensor element. A time-varying point current source is applied to one end of the primary coil.

For the convenience of parametric modeling, the geometric model and finite element mesh are created via XL, a pre- and post-processor for the general electromagnetics finite element analysis engine, EMAS. Figure 2 shows a central part of an electromagnetic finite element model containing the ground plane, primary and secondary coils, and target. The primary and secondary coils are shown in dark color. 3D elements for surrounding air are not shown.

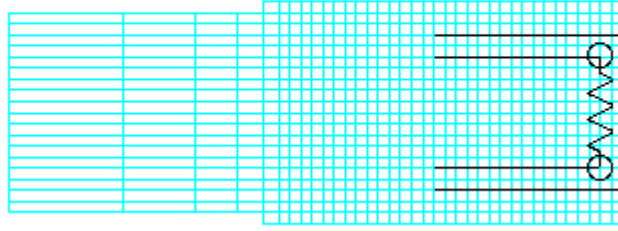


**Fig. 2 Part of an electromagnetic finite element model showing target, ground, wire elements and resistance**

### ***B. Transient analysis***

The transient electromagnetic finite element method solves for the electromagnetic vector potential,  $[A, \Psi]^T$ , via a finite difference procedure. Although the transient solution is unconditionally stable, 10 time steps for the ramp time  $t_0$  are usually required. A ramp current excitation is shown in figure 3.

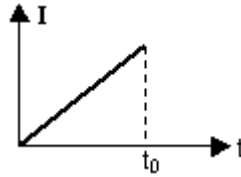


**Fig. 3 Short ramp current excitation**

The secondary output voltage across the loading resistance vs. time are shown in figure 4, where the solid line represents the output when there is no target, and the dash line is the one when fully targeted. The largest output range over the stroke is obtained around  $t/t_0 = 0.2$ .

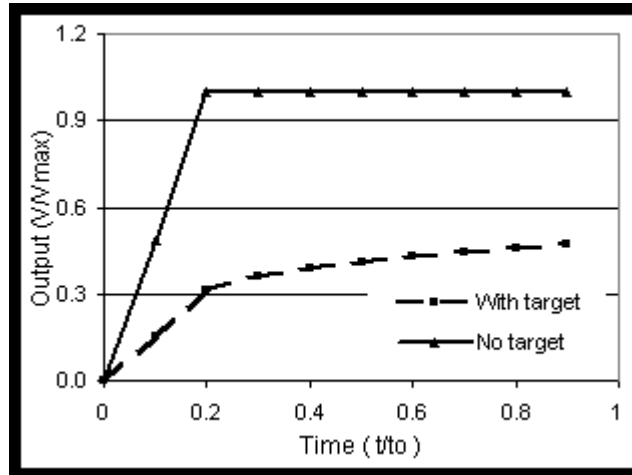


**Fig. 4 Secondary output voltages for no target and fully targeted**

Figure 4 shows that the secondary output remains almost constant after initial rise when there is no target, and creeps over a long period with a target present. To explain this behavior, we need to examine the equivalent circuit equations for the secondary coil and target, which can be written as,

$$M_{1t} \frac{dI_1}{dt} - M_{2t} \frac{dI_2}{dt} = I_t R_t + L_t \frac{dI_t}{dt}, \quad (1)$$

$$M_{12} \frac{dI_1}{dt} - M_{2t} \frac{dI_t}{dt} = I_2 R_2 + L_2 \frac{dI_2}{dt}, \quad (2)$$

where the left hand sides represent the induced potentials. The equivalent lumped circuit parameters at the fundamental operating frequency are evaluated via an AC finite element analysis procedure, and are listed below.

Mutual inductance:  $M_{12} = 6.89$  (nH)  
 $M_{1t} = 8.16$  (nH)  
 $M_{2t} = 5.41$  (nH)

Self inductance:  $L_2 = 11.48$  (nH)  
 $L_t = 2.17$  (nH)

Resistance:  $R_2 = 1.00$  (M $\Omega$ )  
 $R_t = 7.65$  (m $\Omega$ )

in which, the subscripts 1, 2 and t stand for quantities associated with the primary, secondary, and the target respectively. It should be pointed out that these parameters are frequency dependent and are presented only for the purpose of understanding the behavior shown in figure 4 as well as observed in measurement.

The resistances shown above are the effective resistance  $R_t$  in the target, and the total resistance  $R_2$  in the secondary circuit.  $R_2$  includes the coil resistance and the loading resistance. Because  $R_2$  is much larger than  $R_t$ , the current in the secondary circuit  $I_2$  is much smaller than the eddy current  $I_t$  in the target. Thus the term  $M_{2t} dI_t/dt$  is much smaller compared to the first term in Equ. (1), and can be dropped out from the equation. It can be easily shown that the induced eddy current in the target can be approximated by

$$I_t = ce^{-\frac{R_t}{L_t} t} + \frac{M_{1t}}{R_t} \frac{dI_1}{dt} \quad (3)$$

which shows that the eddy current in the target decreases over time due to the time coefficient  $R_t/L_t$  in the target. This implies that the electromagnetic induction in the target decreases, while the induced potential in the secondary increases over time accordingly as indicated at the left hand side of Equ. (2).

This behavior can be further demonstrated by using a permalloy and a superconducting target. The permalloy has a relative magnetic permeability of 2000 and an electric conductivity of  $5.68 \times 10^{10}$  (Siemens/meter), only one tenth that of copper. The superconductor has a conductivity of  $5.8 \times 10^{10}$  (Siemens/meter), which is 1000 times that of copper. Material properties for copper, superconductor and permalloy are listed in table I.

**TABLE I**  
**ELECTROMAGNETIC PROPERTIES OF TARGET MATERIALS**

Material	Conductivity (Siemens/meter)	Relative Permittivity	Relative Permeability
Copper	5.8E7	1	1
Superconductor	5.8E10	1	1
Permalloy	5.8E6	1	2000

Figure 5 shows that a superconductor would be an ideal material for the target because of its effectiveness in induction. Permalloy is not a good choice for this application, because the signal output range over the linear actuating range is reduced.

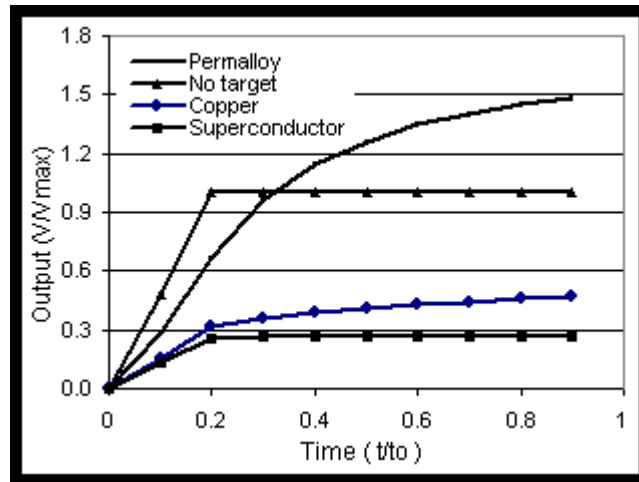


**Fig. 5 Transient output for different target materials**

Transient response from a target made of any typically used metal would fall in between the two responses marked superconductor and permalloy targets as shown in figure 5.

### III. LINEARITY ANALYSIS

Under ideal operating conditions, i.e., at constant operating temperature, with no metallic contamination within the sensor element, etc., the output is expected to be linearly proportional to the target position. However, these conditions are not guaranteed in field applications, and associated errors need to be quantified in advance.

#### A. Temperature error

As indicated in Equ. (3), the time coefficient  $R_t/L_t$  determines the nonlinear behavior of the output signal. As temperature changes, so does the resistance and consequently the eddy current in the target. As a result, the secondary output changes with temperature as well. The resistance (resistivity) of a conductor varies with the temperature and can be written as

For copper having a conductivity of 100% of the International Annealed Copper Standard,  $\alpha_{20} = 0.00393$  and temperatures are in Celsius. The conductivity, which is the inverse of resistivity, is listed in table II for several temperatures within the sensor operating temperature range. When a target is displaced by 0.5mm, the output variations at those temperatures are also listed in table II.

**TABLE II**  
**Conductivity and output at several temperatures**

Temperature (°C)	Conductivity (Siemens/m)	Output (mV)
-40	7.6E7	1.901
-10	6.6E7	1.884
20	5.8E7	1.866
80	4.7E7	1.826
140	3.9E7	1.785

The error due to temperature change is shown in figure 6.

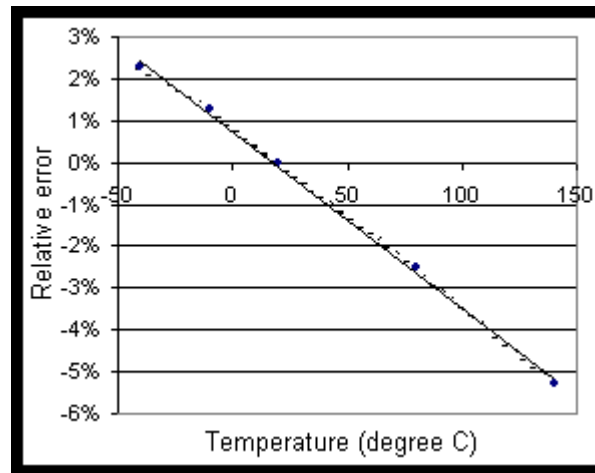


Fig. 6 Output error due to temperature

At the maximum operating temperature (140 °C), the relative error is -5.3 %. If a linear temperature error compensation is used, the relative error after compensation is only 0.19% at the maximum operating temperature.

### B. Contamination error

Electromagnetic materials contaminating the sensor element will also have an effect on the output signal. The worst situation is when a metallic particle falls on a PCB and within the secondary coil. Typical metallic contaminations are copper, steel, and aluminum. Magnetically conducting material provides an efficient path for the magnetic flux, therefore it would strengthen the output signal. In many cases, a magnetically conducting material, in this case, steel, is also an electrically conducting material, therefore it acts in both ways.

Calculated output voltages for a sensor with a copper, aluminum or steel particle in the middle of the secondary are listed in table III. The particle size is  $1 \times 0.5 \times 0.5 \text{ mm}^3$ .

**TABLE III**  
**EFFECT OF CONTAMINATED METALLIC MATERIALS**

Material	Output (mV)	Effect (mV)	Error (%)
No Contamination	6.056		
Copper	6.050	-0.006	-0.10%
Aluminum	6.053	-0.003	-0.05%
Steel	6.065	0.009	0.15%

### C. Results

The experimentally measured results for this sensor element are shown in figure 7. In the range of interest,  $0 < d/d_s < 1$ , the output as a function of position is indeed linear, as predicted by the FEA model.

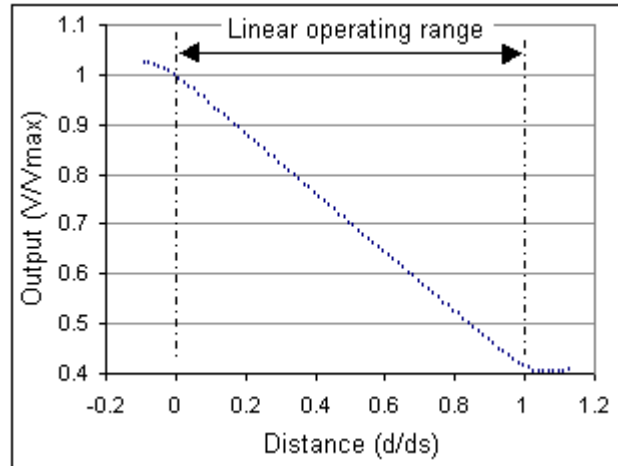


Fig. 7 Measured output vs. target distance showing a linear operating range

## **IV. CONCLUSIONS**

Transient electromagnetic finite element analysis results are applied in designing high frequency inductive position sensors. Electromagnetic FEA has helped us to understand the sensor's nonlinear behavior, and to optimize its design.

## **V. REFERENCES**

1. J. R. Brauer, EMAS Users Manual, Ansoft Corp., 1997
2. W. D. Rolph, Visualizing Electromechanical Design: Finite Element Analysis Supporting the Design Process, Texas Instruments Technical Journal, September-October 1989, pp 24-33
3. L. Huang, R. Mandeville and W. D. Rolph, Electromagnetics and Coupled Structural Finite Element Analysis, Computers & Structures, Vol. 72, 1999, pp 199-207
4. H. F. Tiersten, A Development of Equations of Electromagnetism in Material Continua, Springer-Verlag, 1990
5. W. K. H Panofsky and M. Phillips, Classical Electricity and Magnetism, Addison-Wesley, 1956
6. J.M. Jin, The Finite element method in electromagnetics, John Wiley & Sons, Inc., 1993
7. W. H. Hayt, Engineering Electromagnetics, 5th ed., McGraw-Hall, 1989